

RESEARCH

Open Access



Post-treatment benign changes versus recurrence in non-lymphoid head and neck malignancies: can diffusion-weighted magnetic resonance imaging end up the diagnostic challenge?

Dalia K. Serour^{1*}, Khaled M. Adel¹ and Ayman M. A. Osman²

Abstract

Background: The aim of this prospective cohort study is to substantiate the added value of diffusion-weighted magnetic resonance imaging (DW-MRI) over conventional MRI assessment in the differentiation between locoregional recurrence/residual tumour and post-treatment benign changes in patients with non-lymphoid head and neck malignancies.

Thirty adult patients, each with a suspicious lesion on post-treatment imaging scans at the primary site of a previously treated non-lymphoid head and neck malignancy, were evaluated by MRI and diffusion-weighted imaging (DWI). The apparent diffusion coefficient (ADC) values of the lesions were calculated.

Results: Diffusion-weighted MRI yielded an accuracy of 90%, a sensitivity of 88.9%, a specificity of 91.7%, a positive predictive value of 94.1% and a negative predictive value of 84.6%. The mean ADC value of the lesions was lower in the “locoregional recurrence/residual tumour” group ($1.08 \times 10^{-3} \text{ mm}^2/\text{s}$) compared to the “post-treatment benign changes” group ($1.95 \times 10^{-3} \text{ mm}^2/\text{s}$); $P < 0.001$. An ADC cutoff value of $1.43 \times 10^{-3} \text{ mm}^2/\text{s}$ achieved the same accuracy as the visual assessment by DW-MRI.

Conclusion: Incorporating the DWI sequence into the post-treatment imaging assessment protocol brings a substantial added value to conventional MRI assessment in patients with non-lymphoid head and neck malignancies. This valuable merit of DW-MRI can help avoid or, at least, largely minimize unnecessary or unfeasible tissue sampling. An ADC cutoff value of $1.43 \times 10^{-3} \text{ mm}^2/\text{s}$ can also be utilized to aid in the assessment process.

Keywords: Diffusion-weighted magnetic resonance imaging, Head and neck, Non-lymphoid malignancies, Recurrence, Post-treatment benign changes, Apparent diffusion coefficient

Background

Head and neck cancers collectively represented around 7% of all newly diagnosed cancers worldwide in 2018 [1]. The usual pre-treatment radiological assessment for malignant head and neck tumours involves ultrasonography,

computed tomography (CT) and magnetic resonance imaging (MRI) [2]. However, in the post-treatment phase, imaging assessment of lesions occurring at the primary sites of previously treated head and neck malignancies can be quite difficult owing to the potential distortion of the already anatomically dense region as an effect of surgery or due to post-radiation fibrosis. Furthermore, post-treatment, tissues exhibit changes that can mimic tumour recurrence on standard MRI techniques, thereby eliciting

* Correspondence: daliakhaled80@yahoo.com

¹Department of Diagnostic and Interventional Radiology, Faculty of Medicine, Cairo University, Cairo 11562, Egypt
Full list of author information is available at the end of the article

the need for biopsy as a conclusive method to reach a definitive diagnosis [3]. Biopsy—being an invasive technique—can be erroneous or, in some cases, problematic to the patient.

Diffusion-weighted imaging (DWI) relies on detecting the motion of water molecules across tissues. The degree of diffusion is affected by the composition of the tissue. A variety of factors can, thus, play a role in determining the degree of signal attenuation, e.g. degree of cellularity, integrity of cellular membranes and possible pathophysiological events happening to the tissue [4]. From different series with different b values, an apparent diffusion coefficient (ADC) map can be generated with ADC values for each pixel of the image. Malignant lesions are typically expected to exhibit lower ADC values, whereas post-treatment benign changes usually exhibit higher values [5].

Over the past few years, investigating the role of DWI in evaluating possible tumour recurrences following treatment of head and neck malignancies has been the focus of several studies, with promising results. However, faulty DWI interpretations still exist; variations in the ranges of ADC measurements have been demonstrated by several studies; and different ADC cutoff values, with different accuracies, have been postulated in order to differentiate recurrent/residual malignant lesions from post-treatment benign changes in the head and neck region [6–11]. Hence, research in this particular area is still ongoing in attempts to end up the incompletely resolved diagnostic dilemma of “post-treatment head and neck lesions”. To help with this ongoing research, we carried out a prospective cohort study in order to substantiate the added value of diffusion-weighted MRI (DW-MRI) over conventional MRI assessment in the differentiation between locoregional recurrence/residual tumour and post-treatment benign changes in patients with non-lymphoid head and neck malignancies, as well as to determine and investigate an ADC cutoff value that can potentially be utilized to aid in the assessment process.

Methods

Thirty consecutive adult patients who underwent treatment for non-lymphoid head and neck malignancies, (surgery, chemoradiation or combined surgery and chemo/radiotherapy), between October 2018 and October 2019, then each of whom developed a suspicious lesion on post-treatment MRI scans at the primary site of the previously treated tumour, were enrolled into the study. Patients were selected on the basis of strict inclusion criteria (age of ≥ 18 years at the time of treatment initiation; completion of treatment at least 3 months, but not more than a year, before post-treatment imaging scans were carried out) and exclusion criteria (head and neck lymphomas: non-compliance to treatment and/or imaging assessment). Informed consent was obtained

from all patients before any data or scans were gathered or performed. The study protocol was approved by the institutional Ethical Committee.

Patient factors (age, gender), anatomical locations of the primary tumours, their histopathological types and types of treatment received were all recorded. In all cases, conventional MRI scans were performed along with DWI. The scans were conducted on a Philips 1.5 Tesla MRI machine using a head and neck surface coil. The conventional MRI protocol included T1-weighted images (T1WIs), T2-weighted images (T2WIs) and short tau inversion recovery (STIR) images. The field of view (FOV) was 220 mm. Diffusion scans were acquired via a single-shot echo-planar imaging (EPI) setup at b values of 0–1000 s/mm³. All the acquired images were used to generate an ADC map. T1-weighted post-contrast images were then obtained using gadoteric acid at an injection rate of 2 ml/s. Regions of interests (ROIs) were placed on diffusion-weighted (DW) images and copied to the ADC maps to calculate the ADC values of the suspicious lesions. In every case, the ROI was placed on the margins of the lesion, avoiding any necrotic parts, to encompass the entire viable suspected tumour tissue only. This process of measurement was repeated 3 times, and the average ADC value of the lesion was calculated. The sizes of the lesions were recorded as well. In every case in this study, images were interpreted, independently, by two radiology consultants, each with more than 10 years of experience. Of the two consultants, one interpreted all images in all the study patients, whereas the second varied from one case to the other. The overall agreement between the reporting radiologists was 93.3% (28/30 cases). Only in the case of dispute (2/30 cases), the opinion of a third consultant was obtained. All the reporting radiologists were blinded to the patients' data (including location of primary tumours, their histopathological types and types of treatment received) at the time of interpreting the images.

In all cases, the final definitive diagnosis of the nature of the suspicious lesion was obtained by biopsy [whether using flexible fiberoptic nasopharyngolaryngoscopy, fine-needle aspiration cytology (FNAC) or open surgical biopsy] and histopathological examination. Patients were then divided into two groups [“locoregional recurrence/residual tumour” group and “post-treatment benign changes” group]. The mean ADC values of the lesions in both groups were calculated. Receiver–operating characteristic (ROC) curve analysis was then used to determine an ADC cutoff value that can be utilized to predict the nature of the lesions. Data was analysed using the Statistical Package for Social Sciences (SPSS) software for Windows version 23.

Results

The study patients ranged in age from 23 to 72 years (mean, 43.9 years), with a male-to-female ratio of 4:1. The anatomical locations of the primary malignant head

and neck tumours in the study patients included the nasopharynx ($n = 10$), nose and paranasal sinuses ($n = 7$), oral cavity and oropharynx ($n = 5$), salivary glands ($n = 4$), cheeks ($n = 3$) and larynx ($n = 1$). The histopathological types of the primary tumours included squamous cell carcinoma ($n = 21$), sarcoma ($n = 3$), adenoid cystic carcinoma ($n = 2$), mucoepidermoid carcinoma ($n = 2$) and adenocarcinoma ($n = 2$). The types of treatment received were surgery (resection of the tumour with or without neck dissection) ($n = 8$) and chemoradiation ($n = 9$), as well as combined surgery and chemo/radiotherapy ($n = 13$) (Table 1). Post-treatment MRI scans were requested in the study patients on the basis of symptoms suggestive of recurrent disease and/or abnormal findings on clinical examination ($n = 12$) or as a part of the post-treatment follow-up protocol ($n = 18$).

In all cases, MRI scans revealed a suspicious lesion at the primary site of the previously treated tumour. The average sizes of the lesions in the study group ranged from 0.75 to 4.46 cm (mean, 1.88 cm). Biopsies [using flexible fiberoptic nasopharyngolaryngoscopy ($n = 19$), open surgical biopsy ($n = 9$), FNAC ($n = 2$)] and histopathological examinations revealed that 18/30 lesions (60%) were “locoregional recurrence/residual tumour” and 12/30 lesions (40%) were “post-treatment benign changes”.

The imaging assessments that were based on magnetic resonance (MR) images alone, (T1WIs, T2WIs, STIR

and post-contrast T1-weighted images), were able to characterize the lesions correctly in 22/30 cases (73.3%) (15 cases of “locoregional recurrence/residual tumour” and 7 cases of “post-treatment benign changes”). However, in 8 cases (26.7%), an accurate correct diagnosis was not reached. Hence, conventional MRI assessment yielded an accuracy of 73.3%, a sensitivity of 83.3% and a specificity of 58.3%. On the other hand, the imaging assessments that were based on both MR and DW images were able to correctly predict the nature of the lesions in 27/30 cases (90%). In 17/30 cases (56.7%), the lesions showed noticeable restriction on DW images with corresponding dark signal intensity on the ADC map. Sixteen of those lesions were proven by histopathological examination to be malignant, locoregional recurrence/residual tumour, whereas 1 lesion was proven to be benign, post-treatment benign changes. In the remaining 13 cases (43.3%), the lesions showed no or faint restriction on DW images with corresponding high signal intensity on the ADC map. Eleven of those lesions were proven by histopathological examination to be benign, post-treatment benign changes, whereas 2 lesions were proven to be malignant, locoregional recurrence/residual tumour. Hence, overall, DW-MRI yielded an accuracy of 90%, a sensitivity of 88.9%, a specificity of 91.7%, a positive predictive value (PPV) of 94.1% and a negative predictive value (NPV) of 84.6% (Table 2; Figs. 1, 2 and 3).

In 3/30 cases in this study (10%), the lesions were falsely diagnosed by DW-MRI. In one of those cases, the diagnosis was false-positive, i.e. the lesion was wrongly interpreted as “locoregional recurrence/residual tumour”. This lesion (0.91 cm), which represented benign post-chemoradiation sequelae, exhibited restricted diffusion with a dark signal intensity on the ADC map and a relatively low ADC value. However, the pathology report of the lesion biopsy came back as negative for malignancy and determinate of its benign nature (Fig. 4). In the other two cases, the diagnosis was false-negative, i.e. the lesions were wrongly interpreted as “post-treatment benign changes” while proven by histopathological examination to be malignant. Of those 2 lesions, one had a mixed signal intensity on DW images, and the majority of it displayed the appearance of liquefactive necrosis with associated oedema. The average size of the lesion was 1.42 cm and its ADC value was higher than those of most of other recorded malignant lesions in the study group. The second false-negative lesion (1.31 cm) had a faint restriction on DWI and the corresponding ADC map, while displaying the appearance of ill-defined sheets at the operative bed. It is likely that tissue oedema had confounded the assessment of that lesion in particular (Figs. 5 and 6).

In the “locoregional recurrence/residual tumour” group, the ADC values of the lesions ranged from $0.81 \times 10^{-3} \text{ mm}^2/\text{s}$ to $1.44 \times 10^{-3} \text{ mm}^2/\text{s}$ (mean, $1.08 \times 10^{-3} \text{ mm}^2/\text{s}$),

Table 1 Description of the study patients ($n = 30$)

	Number
Gender	
Male	24
Female	6
Histopathology of the primary tumour	
Squamous cell carcinoma	21
Sarcoma	3
Adenoid cystic carcinoma	2
Mucoepidermoid carcinoma	2
Adenocarcinoma	2
Anatomical location of the primary tumour	
Nasopharynx	10
Nose and paranasal sinuses	7
Oral cavity and oropharynx	5
Cheeks	3
Salivary glands	4
Larynx	1
Treatment received	
Surgery	8
Chemoradiation	9
Combined surgery and chemo/radiotherapy	13

Table 2 Magnetic resonance imaging (MRI) assessment and combined qualitative assessment by MRI and diffusion-weighted imaging (DWI)

Diagnosis	Conventional MRI assessment	Combined qualitative assessment by MRI and DWI	Biopsy and histopathological examination
Locoregional recurrence/residual tumour	20 cases 15 true positive 5 false positive	17 cases 16 true positive 1 false positive	"18 cases"
Post-treatment benign changes	10 cases 7 true negative 3 false negative	13 cases 11 true negative 2 false negative	"12 cases"
Total	30 cases	30 cases	"30 cases"

Results of conventional magnetic resonance imaging (MRI) assessment and combined qualitative assessment by MRI and diffusion-weighted imaging (DWI) compared to the final definitive diagnoses obtained by biopsies and histopathological examinations

MRI magnetic resonance imaging, DWI diffusion-weighted imaging

whereas in the "post-treatment benign changes" group, the ADC values ranged from $1.15 \times 10^{-3} \text{ mm}^2/\text{s}$ to $2.57 \times 10^{-3} \text{ mm}^2/\text{s}$ (mean, $1.95 \times 10^{-3} \text{ mm}^2/\text{s}$). Hence, the mean ADC value was lower in the "locoregional recurrence/residual tumour" group compared to the "post-treatment benign changes" group, and the difference was statistically significant ($P < 0.001$) (Fig. 7).

Receiver–operating characteristic (ROC) curve analysis showed that, among the investigated ADC cutoff values, the cutoff value of $1.43 \times 10^{-3} \text{ mm}^2/\text{s}$ was the most accurate for predicting the nature of the suspicious lesions, with an area under the curve of 0.961 (Fig. 8). A diagnosis of "locoregional recurrence/residual tumour" was made if the ADC value of the suspicious lesion was less than or equal to the aforementioned cutoff value. An ADC cutoff value of $1.43 \times 10^{-3} \text{ mm}^2/\text{s}$ was able to correctly predict the nature of the lesions in 27/30 cases, thus achieving the same accuracy as DW-MRI (90%), yet with a sensitivity of 94.4%, a specificity of 83.3%, a PPV of 89.4% and a NPV of 90.9%.

Discussion

In the postoperative or post-radiation phase, tissues at the primary site of a treated malignant tumour exhibit local changes (e.g. oedema, inflammation and fibrosis) that can mimic tumour recurrence or residual tumour tissue on MRI scans through eliciting high signal intensity on T2WIs and post-contrast T1WIs [12]. Noting a suspicious lesion at the site of a treated cancer on post-treatment imaging scans often calls for further evaluation of the said lesion through an invasive approach by acquiring tissue samples for accurate histopathological characterization of the nature of the lesion [13].

Diffusion-weighted imaging can offer an insight into the cellular composition of scanned tissue through displaying varying degrees of signal attenuation. Since tumour tissues are typically more cellular than tissues with post-treatment benign changes, differences in the degrees of signal attenuation on DWI and in ADC values are expected [13]. In the head and neck region, the use of DWI is becoming increasingly popular nowadays as

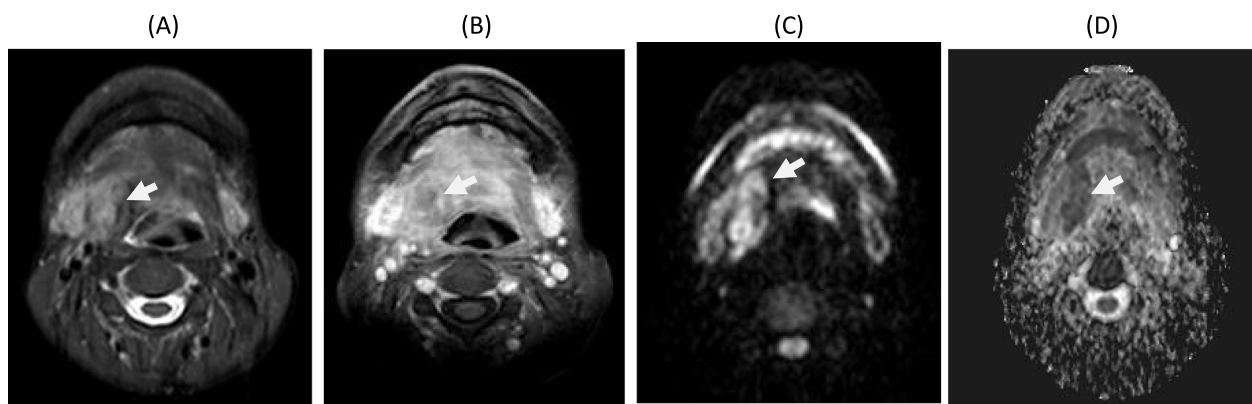


Fig. 1 Pathologically proven recurrent squamous cell carcinoma of the tongue following surgical resection and adjuvant radiotherapy. **a** Axial fat-saturated T2-weighted image (T2WI) showing an ill-defined lesion of intermediate-to-high signal intensity at the operative bed (right side of the tongue). **b** Axial fat-saturated T1-weighted image (T1WI) post-contrast sequence showing faint, ill-defined, inhomogeneous enhancement of the lesion. **c** Diffusion-weighted imaging (b1000) revealing the hyperintense pattern of the lesion. **d** Apparent diffusion coefficient (ADC) map revealing the hypointense pattern of the lesion, with a mean ADC value of $1.21 \times 10^{-3} \text{ mm}^2/\text{s}$ suggestive of tumour recurrence

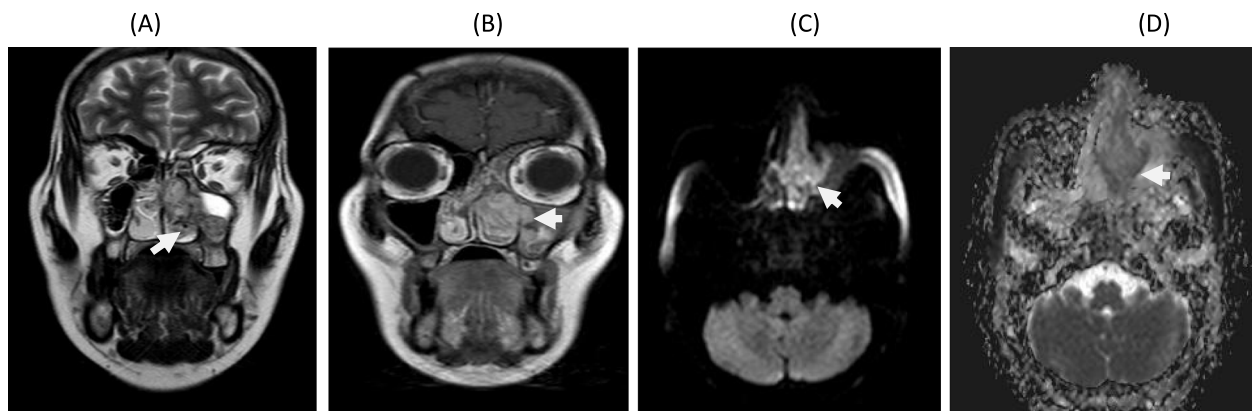


Fig. 2 Pathologically proven recurrent spindle cell sarcoma of the left maxilla following chemoradiation. **a** Coronal T2-weighted image (T2WI) showing a newly developed lesion of intermediate-to-low signal intensity at the left maxillary antrum and nasal cavity. **b** Coronal T1-weighted image (T1WI) post-contrast sequence showing inhomogeneous enhancement of the lesion. **c** Diffusion-weighted imaging (b1000) revealing the hyperintense pattern of the lesion. **d** Apparent diffusion coefficient (ADC) map revealing the hypointense pattern of the lesion, with a mean ADC value of $1.01 \times 10^{-3}/\text{mm}^2$ suggestive of tumour recurrence

opposed to the past where motion and magnetic susceptibility artifacts were more pronounced [14].

In the current study, DW-MRI has proved superior to conventional MRI assessment in terms of diagnostic accuracy, sensitivity and specificity (90%, 88.9% and 91.7% versus 73.3%, 83.3% and 58.3%, respectively). This largely supports the notion that incorporating a DWI protocol in the post-treatment imaging assessment of patients with non-lymphoid head and neck malignancies could have a potentially beneficial role in characterizing the nature of suspicious lesions. The mean ADC value of the lesions was significantly lower in the “locoregional recurrence/residual tumour” group ($1.08 \times 10^{-3} \text{ mm}^2/\text{s}$) compared to the “post-treatment benign changes” group ($1.95 \times 10^{-3} \text{ mm}^2/\text{s}$); $P < 0.001$. This finding is in consonance with the previously

published data which consistently reported that higher ADC values would be expected with post-treatment benign changes while lower ADC values would be expected with recurrent/residual malignant lesions [6–9, 15].

The lesions were falsely diagnosed by DW-MRI in 3/30 cases in this study (10%). In one of those cases, the diagnosis was false-positive, while in the other two, it was false-negative. In DWI, hypercellular tissue (e.g. malignant tissue) often exhibits high signal intensity on the ADC map with high b values (e.g. b1000) resulting in a low ADC value, owing to the limited extracellular space with subsequent restriction to the motion of water molecules. However, this does not mean that all tissues exhibiting high signal intensity on b1000 images are malignant because signal intensity is influenced both by

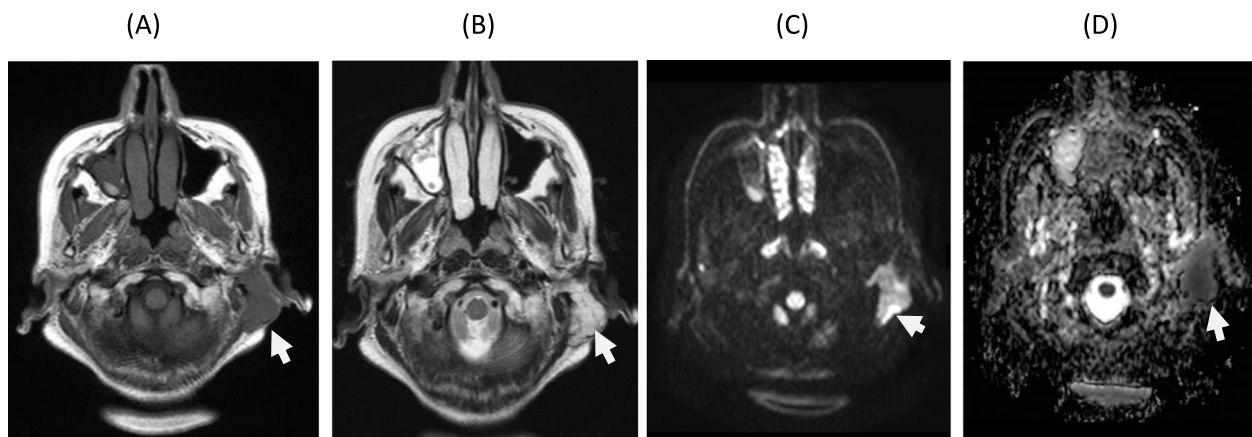


Fig. 3 Pathologically proven recurrent adenoid cystic carcinoma of the left parotid gland following parotidectomy and adjuvant radiotherapy. **a** Axial T1-weighted image (T1WI) showing a well-defined lesion of low signal intensity at the operative bed of the previous left parotidectomy. **b** Axial T2-weighted image (T2WI) showing the high signal intensity of the lesion. **c** Diffusion-weighted imaging (b1000) revealing the hyperintense pattern of the lesion. **d** Apparent diffusion coefficient (ADC) map revealing the hypointense pattern of the lesion, with a mean ADC value of $0.96 \times 10^{-3}/\text{mm}^2$ suggestive of tumour recurrence

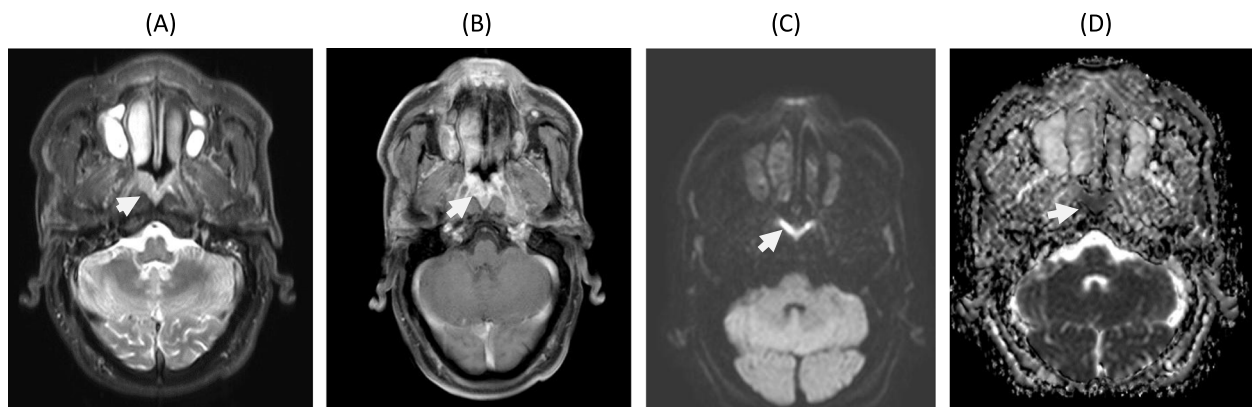


Fig. 4 Pathologically proven post-treatment benign changes following chemoradiation for nasopharyngeal carcinoma. In this case, biopsy and histopathological examination revealed tissue fibrosis with no malignancy. However, the lesion was falsely diagnosed by diffusion-weighted imaging (DWI), i.e. wrongly interpreted as “locoregional recurrence/residual tumour”. **a** Axial T2-weighted image (T2WI) showing an area of diffuse thickening within the posterior nasopharyngeal wall, being more prominent on the right side, with intermediate signal intensity. **b** Axial T1-weighted image (T1WI) post-contrast sequence showing inhomogeneous enhancement of the lesion. **c** Diffusion-weighted imaging (b1000) revealing the hyperintense pattern of the lesion. **d** Apparent diffusion coefficient (ADC) map revealing the hypointense pattern of the lesion, with a mean ADC value of $1.44 \times 10^{-3}/\text{mm}^2$ suggestive of tumour recurrence

the motion-probing gradient-induced signal loss and the original T2-weighted signal. Hence, in benign tissue (e.g. fibrous tissue), even in the case of strong signal decay, a hyperintensity at b1000 may remain. This remaining signal at b1000, referred to as the “T2 shine-through” effect, is difficult to differentiate from the hyperintensity observed in malignant tissues with restricted diffusion.

Such effect can be minimized by using higher b values, but most often cannot be completely abolished [16]. This could explain the false-positive case in the current study. On the other hand, in recurrent/residual malignant lesions, the relatively high ADC values that may lead to faulty interpretations as “post-treatment benign changes” might be related to the presence of oedema and post-radiation liquefactive

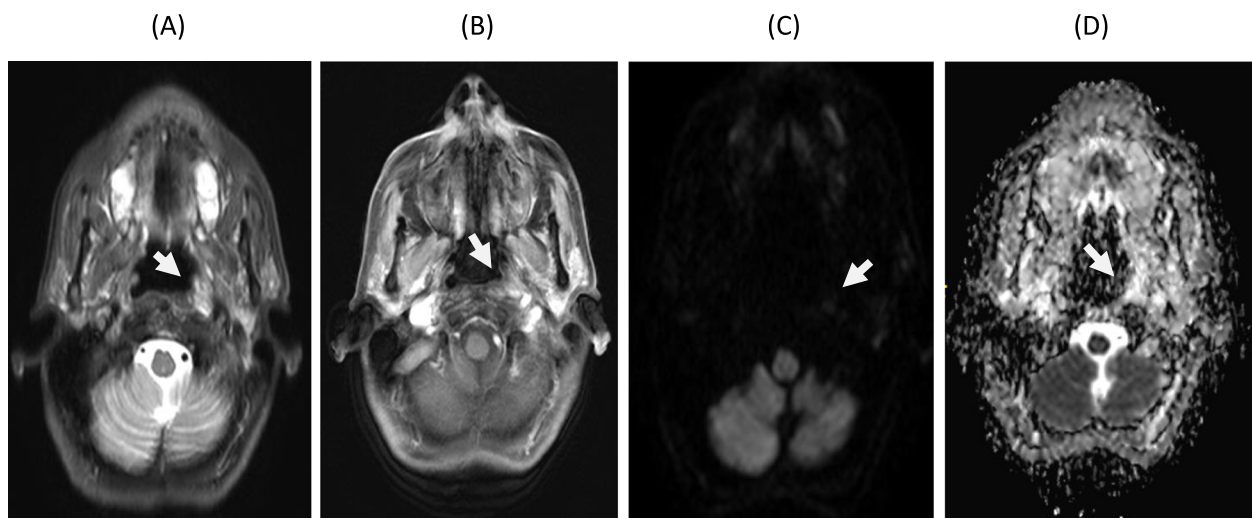


Fig. 5 Pathologically proven recurrent nasopharyngeal carcinoma following radiotherapy. In this case, biopsy and histopathological examination revealed nasopharyngeal carcinoma. However, the lesion was falsely diagnosed by diffusion-weighted imaging (DWI), i.e. wrongly interpreted as “post-treatment benign changes”. **a** Axial T2-weighted image (T2WI) showing a left nasopharyngeal thickening, with high signal intensity. **b** Axial fat-saturated T1-weighted image (T1WI) post-contrast sequence showing faint, inhomogeneous, enhancement of the lesion. **c** Diffusion-weighted imaging (b1000) revealing the intermediate-to-low signal intensity pattern of the lesion. **d** Apparent diffusion coefficient (ADC) map revealing the mixed, intermediate-to-high, signal intensity pattern of the lesion, with a mean ADC value of $1.43 \times 10^{-3}/\text{mm}^2$; possibility of post-treatment benign changes, rather than tumour recurrence, was considered

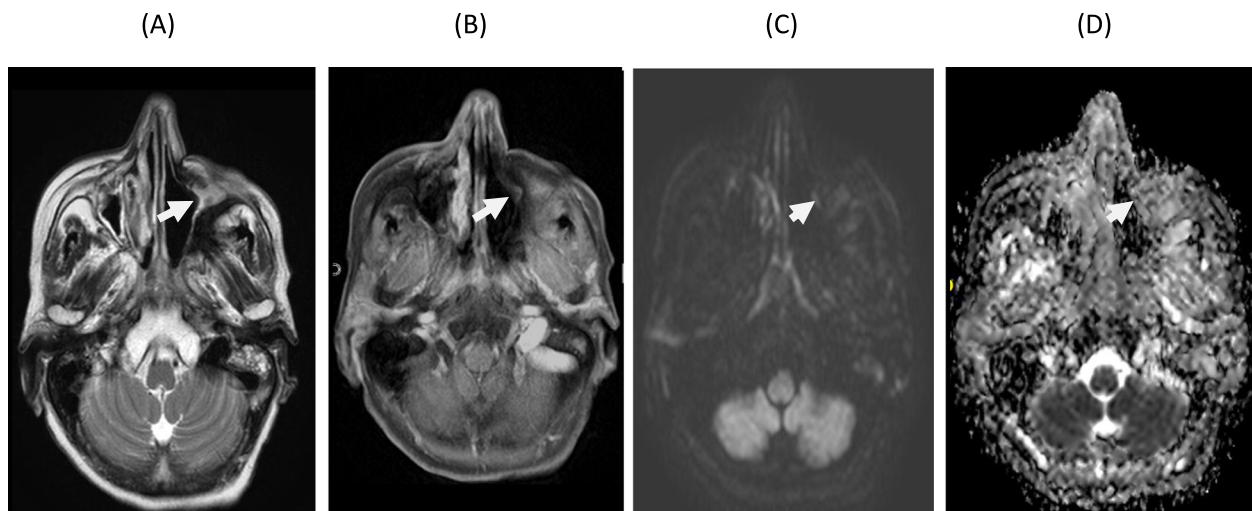


Fig. 6 Pathologically proven recurrent adenoid cystic carcinoma of the left maxilla following surgical resection and adjuvant chemoradiation. In this case, biopsy and histopathological examination revealed adenoid cystic carcinoma. However, the lesion was falsely diagnosed by diffusion-weighted imaging (DWI), i.e. wrongly interpreted as “post-treatment benign changes”. **a** Axial T2-weighted image (T2WI) showing a rather oblong sheet of high signal intensity at the operative bed (left maxilla). **b** Axial fat-saturated T1-weighted image (T1WI) post-contrast sequence showing faint, rather homogenous, enhancement of the lesion. **c** Diffusion-weighted imaging (b1000) revealing the intermediate-to-low signal intensity pattern of the lesion. **d** Apparent diffusion coefficient (ADC) map revealing the mixed, intermediate-to-high, signal intensity pattern of the lesion, with a mean ADC value of $1.39 \times 10^{-3}/\text{mm}^2$; possibility of post-treatment benign changes was considered

necrosis [17]. This could explain the false-negative cases in the study. Moreover, in the three cases that were falsely diagnosed by DW-MRI, the relatively small sizes of the lesions might have partially influenced the visual imaging assessment outcomes.

Looking at the ranges of the ADC measurements in this study, an overlap between the ranges of the two study groups can be clearly noticed. This finding is in consonance with the previously mentioned similar research by Jajodia et al. [6] where faulty interpretation by

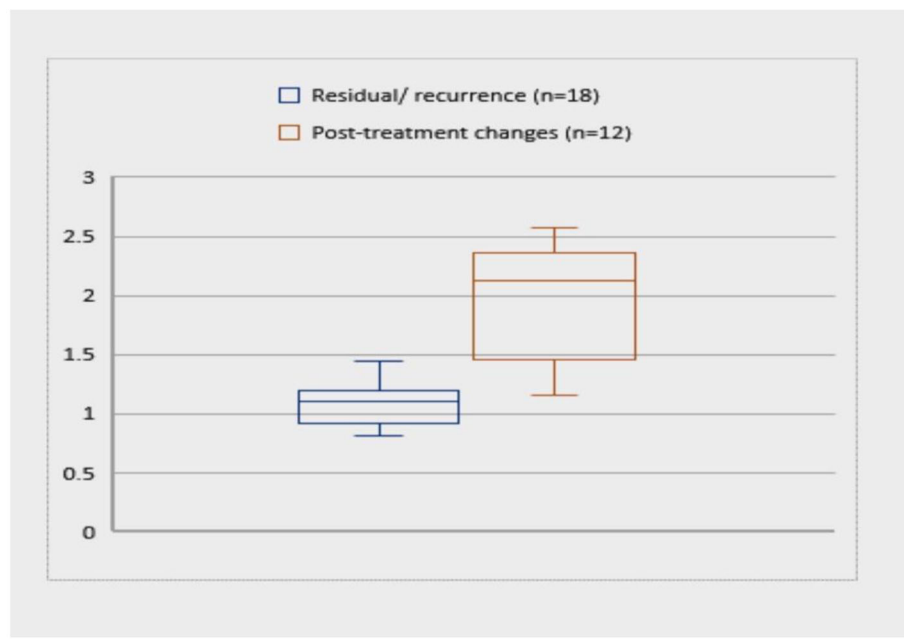


Fig. 7 Box and whisker plot. The plot shows the apparent diffusion coefficient (ADC) values of the suspicious lesions in the two study groups, with most of the lesions in the “locoregional recurrence/residual tumour” group exhibiting significantly lower ADC values than those in the “post-treatment benign changes” group

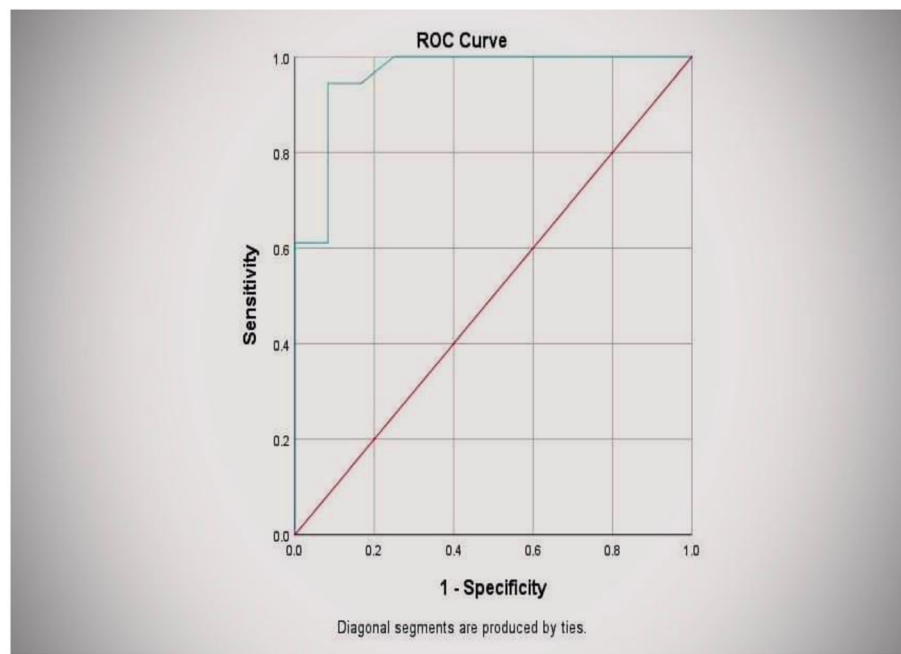


Fig. 8 Receiver–operating characteristic (ROC) curve analysis. The ROC curve analysis shows that the apparent diffusion coefficient (ADC) cutoff value of $1.43 \times 10^{-3} \text{ mm}^2/\text{s}$ was the most accurate for predicting the nature of the suspicious lesions, with an area under the curve of 0.961, a sensitivity of 94.4% and a specificity of 83.3%

DWI, as well as an overlap between the ranges of the ADC measurements, has also been demonstrated. It is hypothesized that this overlap could be due to the inclusion of different anatomical locations as well as different histopathological types of the primary tumours. Similar overlaps were noted in other studies with different tumour sites, as shown in the study conducted by Hein et al. [10]. Possibly, with more data being gathered on specific anatomical locations in the head and neck region, a more defined and accurate range of ADC measurements—possibly also specific for each tumour type—could be obtained. It is also worth pointing out that, besides the varying anatomical locations and the heterogeneity of the malignant tumours included, the variability in the recorded ADC measurements between different studies could also be attributed to the variability in the ROI placement methods, where some authors adopt the freehand tool while others rely on point or region measurement. Modifications to the DWI technique have been suggested by some researchers in order to nullify the equipment-related aspect of measurement variability. Vidiri et al. [18] have suggested the use of smaller FOV for a more accurate ADC measurement. Meanwhile, Koontz et al. [11] have devised a tool to bypass the variability in the ADC measurements they have tested, with promising results. Several authors have also investigated the advantages of using high b values (e.g. $b2000$) in the assessment of post-treatment head and neck lesions [19–22].

Furthermore, it has been suggested that the overlap between the ranges of the ADC measurements can potentially be patched by integrating the DWI along with positron emission tomography/computed tomography (PET/CT) to help in the assessment process. Alternatively, positron emission tomography/magnetic resonance imaging (PET/MRI) can serve as a replacement to PET/CT in the head and neck region [23–25].

In the present study, quantitative assessment using an ADC cutoff value of $1.43 \times 10^{-3} \text{ mm}^2/\text{s}$ has proved to be of similar accuracy as the visual qualitative assessment by DW-MRI (90%), but with higher sensitivity and NPV. This slightly disagrees with the recent series by Jajodia et al. [6] which reported a slight difference in the diagnostic power between ADC measurement and visual assessment by DW-MRI, in favour of the latter. Yet, this difference might have not been demonstrated in the current study due to the relatively limited number of patients.

Fellow research groups had postulated different ADC cutoff values in order to differentiate recurrent/residual malignant lesions from post-treatment benign changes in the head and neck, with different accuracies. Desouky and colleagues [7] demonstrated 100% sensitivity and 74% specificity when using an ADC cutoff value of $0.96 \times 10^{-3} \text{ mm}^2/\text{s}$ for differentiating recurrent squamous cell carcinomas from post-treatment changes in the region of the larynx only. Other authors, however, proposed slightly higher ADC cutoff values. For example, Vaid et al. [8]

attained 90.13% sensitivity and 82.5% specificity when using a cutoff value of $1.2 \times 10^{-3} \text{ mm}^2/\text{s}$ to differentiate between a variety of post-treatment lesions at different sites in the head and neck in a heterogeneous group of patients as regards the histopathology of their primary cancers. Similarly, an ADC value of $1.3 \times 10^{-3} \text{ mm}^2/\text{s}$ contributed to the best results when it was used as a cutoff value by Razek et al. [9] (84% sensitivity/90% specificity) and Jajodia et al. [6] (94% sensitivity/83.3% specificity).

The current study was not without limitations. Of course, the small sample size was the main drawback. Other limitations included patient heterogeneity, as regards locations of primary tumours, their histopathological types and types of treatment received, and selection bias, where some patients, e.g. thyroid cancer patients, were not included in the sampled population, while others, e.g. laryngeal cancer patients, were included but in small numbers that do not accurately represent their true incidence in the target population. This bias was attributed mainly to the consecutive enrollment of patients into the study.

Conclusions

Incorporating the DWI sequence into the post-treatment imaging assessment protocol brings a substantial added value to conventional MRI assessment in patients with non-lymphoid head and neck malignancies and can have a potentially beneficial role in evaluating possible tumour recurrences/residual tumours in those patients. This valuable merit of DWI can help avoid or, at least, largely minimize unnecessary or unfeasible tissue sampling. Furthermore, an ADC cutoff value of $1.43 \times 10^{-3} \text{ mm}^2/\text{s}$ can yield similar results to the visual assessment by DW-MRI and can, thus, potentially be utilized to aid in the assessment process. Studies with larger sample sizes, more standardized protocols and higher levels of patient homogeneity—as regards anatomical locations and histopathology of primary tumours—are still needed in order to bring about a more accurate range of ADC measurements and, consequently, more accurate and reliable results.

Abbreviations

CT: Computed tomography; MRI: Magnetic resonance imaging; DWI: Diffusion-weighted imaging; ADC: Apparent diffusion coefficient; DW-MRI: Diffusion-weighted magnetic resonance imaging; T1WIs: T1-weighted images; T2WIs: T2-weighted images; STIR: Short tau inversion recovery; FOV: Field of view; EPI: Echo-planar imaging; ROIs: Regions of interests; DW: Diffusion-weighted; FNAC: Fine-needle aspiration cytology; ROC: Receiver–operating characteristic; SPSS: Statistical Package for Social Sciences; MR: Magnetic resonance; PPV: Positive predictive value; NPV: Negative predictive value; PET/CT: Positron emission tomography/computed tomography; PET/MRI: Positron emission tomography/magnetic resonance imaging

Acknowledgements

Not applicable.

Authors' contributions

DS formulated the research goals, designed the study methodology and supervised/actively participated in the research activity planning/execution.

KA conducted/actively participated in the research process, performed the data collection/data analysis and wrote the initial draft of the manuscript. AAO actively participated in the research activity execution, assisted in the data analysis and largely contributed in reviewing/editing and writing of the manuscript. The authors read and approved the final manuscript.

Funding

This research did not receive any specific grant from funding agencies in the public, commercial or not-for-profit sectors. There were no sources of funding for this work other than departmental resources.

Availability of data and materials

The datasets used and/or analysed during the current study are available from the corresponding author on reasonable request.

Ethics approval and consent to participate

This study was approved by the Research Ethics Committee of the Faculty of Medicine, Cairo University on 3 October 2018. Ethics Committee reference number is not available (was not provided). Written informed consent was obtained from all the study patients before any data or scans were gathered or performed.

Consent for publication

All patients included in this research (≥ 18 years of age) gave written informed consent to publish the data contained within this study. If the patient was unconscious when consent for publication was requested, written informed consent for the publication of data was given by his/her parent or legal guardian.

Competing interests

The authors declare that they have no competing interests.

Author details

¹Department of Diagnostic and Interventional Radiology, Faculty of Medicine, Cairo University, Cairo 11562, Egypt. ²Department of General Surgery, Faculty of Medicine, Cairo University, Cairo 11562, Egypt.

Received: 15 January 2020 Accepted: 30 March 2020

Published online: 14 April 2020

References

1. Bray F, Ferlay J, Soerjomataram I, Siegel RL, Torre LA, Jemal A (2018) Global cancer statistics 2018: GLOBOCAN estimates of incidence and mortality worldwide for 36 cancers in 185 countries. *CA Cancer J Clin* 68(6):394–424. <https://doi.org/10.3322/caac.21492>
2. King AD (2007) Multimodality imaging of head and neck cancer. *Cancer Imaging* 7(Special Issue AN). <https://doi.org/10.1102/1470-7330.2007.9013>
3. Connolly M, Srinivasan A (2018) Diffusion-weighted imaging in head and neck cancer. *Magn Reson Imag Clin N Am* 26(1):121–133. <https://doi.org/10.1016/j.mric.2017.08.011>
4. Verhappen M, Pouwels P, Ljumanovic R, van der Putten L, Knol D, De Bree R et al (2012) Diffusion-weighted MR imaging in head and neck cancer: comparison between half-Fourier acquired single-shot turbo spin-echo and EPI techniques. *AJNR Am J Neuroradiol* 33(7):1239–1246. <https://doi.org/10.3174/ajnr.a2949>
5. Surov A, Meyer HJ, Wienke A (2017) Correlation between apparent diffusion coefficient (ADC) and cellularity is different in several tumors: a meta-analysis. *Oncotarget* 8(35):59492–59499. <https://doi.org/10.18632/oncotarget.17752>
6. Jajodia A, Aggarwal D, Chaturvedi AK, Rao A, Mahawar V, Gairola M et al (2019) Value of diffusion MR imaging in differentiation of recurrent head and neck malignancies from post treatment changes. *Oral Oncol* 96:89–96. <https://doi.org/10.1016/j.oraloncology.2019.06.037>
7. Desouky S, Aboseif S, Shama S, Gaafar A, Gamaleldin O (2015) Role of dynamic contrast enhanced and diffusion weighted MRI in the differentiation between post treatment changes and recurrent laryngeal cancers. *Egy J Radiology Nuc Med* 46(2):379–389. <https://doi.org/10.1016/j.ejrm.2015.01.012>
8. Vaid S, Chandorkar A, Atre A, Shah D, Vaid N (2017) Differentiating recurrent tumours from post-treatment changes in head and neck cancers: does

- diffusion-weighted MRI solve the eternal dilemma? *Clin Radiol* 72(1):74–83. <https://doi.org/10.1016/j.crad.2016.09.019>
9. Razeq AA, Kandeel A, Soliman N, El-shenshawhy HM, Kamel Y, Nada N et al (2007) Role of diffusion-weighted echo-planar MR imaging in differentiation of residual or recurrent head and neck tumors and posttreatment changes. *AJNR Am J Neuroradiol* 28(6):1146–1152. <https://doi.org/10.3174/ajnr.a0491>
 10. Hein P, Eskey C, Dunn J, Hug EB (2004) Diffusion-weighted imaging in the follow-up of treated high-grade gliomas: tumor recurrence versus radiation injury. *AJNR Am J Neuroradiol* 25:201–209
 11. Koontz NA, Wiggins RH (2017) Differentiation of benign and malignant head and neck lesions with diffusion tensor imaging and DWI. *Am J Roentgenol* 208(5):1110–1115. <https://doi.org/10.2214/ajr.16.16486>
 12. King AD, Chow KK, Yu KH, Mo FK, Yeung DK, Yuan J et al (2013) Head and neck squamous cell carcinoma: diagnostic performance of diffusion-weighted MR imaging for the prediction of treatment response. *Radiology* 266(2):531–538. <https://doi.org/10.1148/radiol.12120167>
 13. Hermans R (2010) Diffusion-weighted MRI in head and neck cancer. *Curr Opin Otolaryngol Head Neck Surg* 18(2):72–78. <https://doi.org/10.1097/moo.0b013e32833555f2>
 14. Stadlbauer A, Bernt R, Gruber S, Bogner W, Pinker K, van der Riet W et al (2009) Diffusion-weighted MR imaging with background body signal suppression (DWIBS) for the diagnosis of malignant and benign breast lesions. *Eur Radiol* 19:2349–2356. <https://doi.org/10.1007/s00330-009-1426-2>
 15. Vandecaveye V, Keyzer FD, Nuyts S, Deraedt K, Dirix P, Hamaekers P et al (2007) Detection of head and neck squamous cell carcinoma with diffusion weighted MRI after (chemo)radiotherapy: correlation between radiologic and histopathologic findings. *Int J Radiat Oncol Biol Phys* 67(4):960–971. <https://doi.org/10.1016/j.ijrobp.2006.09.020>
 16. Koh DM, Collins DJ (2007) Diffusion-weighted MRI in the body: applications and challenges in oncology. *AJR Am J Roentgenol* 188(6):1622–1635. <https://doi.org/10.2214/AJR.06.1403>
 17. Matzek W, Czerny C, Krestan C, Shibany N, Linecker A, Imhof H et al (2003) Non-invasive therapy monitoring with diffusion weighted imaging: evaluation of effects of radiochemotherapy in squamous cell carcinomas of the oropharynx. Proceedings of the 16th International Congress of Head & Neck Radiology. Frankfurt, Germany
 18. Vidiri A, Minosse S, Piludu F, Curione D, Pichi B, Spriano G et al (2016) Feasibility study of reduced field of view diffusion-weighted magnetic resonance imaging in head and neck tumors. *Acta Radiol* 58(3):292–300. <https://doi.org/10.1177/0284185116652014>
 19. Hatakenaka M, Shioyama Y, Nakamura K, Yabuuchi H, Matsuo Y, Sunami S, et al (2011). Apparent diffusion coefficient calculated with relatively high b-values correlates with local failure of head and neck squamous cell carcinoma treated with radiotherapy. *AJNR Am J Neuroradiol* 32(10):1904–1910. <https://doi.org/10.3174/ajnr.a2610>
 20. Lambrecht M, Calster BV, Vandecaveye V, De Keyzer F, Roebben I, Hermans R et al (2014) Integrating pretreatment diffusion weighted MRI into a multivariable prognostic model for head and neck squamous cell carcinoma. *Radiother Oncol* 110(3):429–434. <https://doi.org/10.1016/j.radonc.2014.01.004>
 21. Ryoo I, Kim JH, Choi SH, Sohn CH, Kim SC (2015) Squamous cell carcinoma of the head and neck: comparison of diffusion-weighted MRI at b-values of 1,000 and 2,000 s/mm² to predict response to induction chemotherapy. *Magn Reson Med* 14(4):337–345. <https://doi.org/10.2463/mrms.2015-0003>
 22. Hwang I, Choi S, Kim YJ, Kim KG, Lee AL, Yun TJ et al (2013) Differentiation of recurrent tumor and posttreatment changes in head and neck squamous cell carcinoma: application of high b-value diffusion-weighted imaging. *AJNR Am J Neuroradiol* 34(12):2343–2348. <https://doi.org/10.3174/ajnr.a3603>
 23. Kim SG, Friedman K, Patel S, Hagiwara M (2016) Potential role of PET/MRI for imaging metastatic lymph nodes in head and neck cancer. *Am J Roentgenol* 207(2):248–256. <https://doi.org/10.2214/ajr.16.16265>
 24. Lee SJ, Seo HJ, Cheon GJ, Kim JH, Kim EE, Kang KW et al (2013) Usefulness of integrated PET/MRI in head and neck cancer: a preliminary study. *Nucl Med Mol Imaging* 48(2):98–105. <https://doi.org/10.1007/s13139-013-0252-2>
 25. Ryan JL, Aaron VD, Sims JB (2019) PET/MRI vs PET/CT in head and neck imaging: when, why, and how? *Semin Ultrasound CT MR* 40(5):376–390. <https://doi.org/10.1053/j.sult.2019.07.002>

Publisher's Note

Springer Nature remains neutral with regard to jurisdictional claims in published maps and institutional affiliations.

Submit your manuscript to a SpringerOpen[®] journal and benefit from:

- Convenient online submission
- Rigorous peer review
- Open access: articles freely available online
- High visibility within the field
- Retaining the copyright to your article

Submit your next manuscript at ► [springeropen.com](https://www.springeropen.com)